ELSEVIER

Contents lists available at ScienceDirect

Journal of Theoretical Biology

journal homepage: www.elsevier.com/locate/yjtbi



Habitual sleep duration affects recovery from acute sleep deprivation: A modeling study



Sofia H. Piltz ^a, Cecilia G. Diniz Behn ^b. Victoria Booth ^{c,*}

- ^a Department of Mathematics, University of Michigan, Ann Arbor, MI 48109, USA
- ^b Department of Applied Mathematics and Statistics, Colorado School of Mines, Golden, CO 80401
- ^c Departments of Mathematics and Anesthesiology, University of Michigan, Ann Arbor, MI 48109, USA

ARTICLE INFO

Article history: Received 22 January 2020 Revised 27 June 2020 Accepted 4 July 2020 Available online 11 July 2020

Keywords:
Habitual long and short sleepers
Homeostatic sleep drive
Circadian rhythm
Interindividual variability
Sleep deprivation
Computational modeling

ABSTRACT

Adult humans exhibit high interindividual variation in habitual sleep durations, with short sleepers typically sleeping less than 6 h per night and long sleepers typically sleeping more than 9 h per night. Analysis of the time course of homeostatic sleep drive in habitual short and long sleepers has not identified differences between these groups, leading to the hypothesis that habitual short sleep results from increased tolerance to high levels of homeostatic sleep drive. Using a physiologically-based mathematical model of the sleep-wake regulatory network, we investigate responses to acute sleep deprivation in simulated populations of habitual long, regular and short sleepers that differ in daily levels of homeostatic sleep drive. The model predicts timing and durations of wake, rapid eye movement (REM), and non-REM (NREM) sleep episodes as modulated by the homeostatic sleep drive and the circadian rhythm, which is entrained to an external light cycle. Model parameters are fit to experimental measures of baseline sleep durations to construct simulated populations of individuals of each sleeper type. The simulated populations are validated against data for responses to specific acute sleep deprivation protocols. We use the model to predict responses to a wide range of sleep deprivation durations for each sleeper type. Model results predict that all sleeper types exhibit shorter sleep durations during recovery sleep that occurs in the morning, but, for recovery sleep times occurring later in the day, long and regular sleepers show longer and more variable sleep durations, and can suffer longer lasting disruption of daily sleep patterns compared to short sleepers. Additionally, short sleepers showed more resilience to sleep deprivation with longer durations of waking episodes following recovery sleep. These results support the hypothesis that differential responses to sleep deprivation between short and long sleepers result from differences in the tolerance for homeostatic sleep pressure.

© 2020 Elsevier Ltd. All rights reserved.

1. Introduction

The American Academy of Sleep Medicine recommends that adults sleep at least 7 h per night to promote optimal health and wellbeing, but there is a lot of interindividual variation in sleep need (Badr et al., 2015; Van Dongen, 2006). Recently, genetic factors that influence sleep need have been identified (Dauvilliers and Maret, 2005; Franken et al., 2006), but there are likely many other factors including age, sex, and activity levels that affect an individual's sleep requirements. Typically, "short" sleepers have been classified as individuals who habitually sleep less than 6 h per night, and "long" sleepers as those who habitually sleep more

E-mail addresses: piltz@umich.edu (S.H. Piltz), cdinizbe@mines.edu (C.G. Diniz Behn), vbooth@umich.edu (V. Booth).

than 9 h per night. However, formal criteria for the characterization of habitual short and long sleeper types are yet to be determined (Van Dongen et al., 2005). Experiments suggest that differences between total sleep time for habitual short and long sleepers are primarily caused by different amounts of stage 2 sleep and rapid eye movement (REM) sleep (Rusterholz et al., 2010; Aeschbach et al., 1996). However, sleep architecture, including cycling between REM and non-REM (NREM) sleep, is generally conserved across sleeper types. Indeed, it has been shown experimentally that the length of the REM-NREM cycle does not differ between habitual short and long sleepers, but habitual short sleepers have 3-4 REM-NREM cycles per sleep episode while habitual long sleepers have 4-7 REM-NREM cycles per sleep episode (Aeschbach et al., 1996).

There is also evidence that interindividual variability in baseline sleep need affects responses to sleep deprivation. Specifically, sleep

^{*} Corresponding author.

deprivation experiments have documented large variation in interindividual need for recovery sleep as well as metrics of performance and alertness with shorter sleepers typically showing greater resilience to sleep deprivation compared to longer sleepers (Van Dongen, 2006; Aeschbach et al., 2001). However, the connections between baseline sleep need and tolerance for acute or chronic sleep deprivation are not well-understood.

Our modeling study was motivated by two published experiments comparing the responses of different sleeper types under acute sleep deprivation conditions (Benoit et al., 1980; Aeschbach et al., 1996). These studies varied in the behavioral types tested and in the duration of the acute sleep deprivation administered. Namely, Benoit et al. (1980) measured sleep in the first recovery night following 24 and 36 h of wake (i.e., corresponding to approximately 8 and 20 h of sleep deprivation from usual sleep onset, respectively) in participants exhibiting habitual long, regular, and short sleep behaviors. Aeschbach et al. (1996) studied recovery over the first two nights following 24 h of sleep deprivation in participants exhibiting habitual short and long sleep behaviors

Under baseline conditions, both studies reported consistent total sleep times (TST) and REM sleep durations for each observed sleeper type (Benoit et al., 1980; Aeschbach et al., 1996). Mean values of REM sleep durations for long and short sleepers varied between studies (long: 91.8 ± 21.4 mins (Benoit et al., 1980) vs 125.4 ± 26.2 mins (Aeschbach et al., 1996); short: 48.9 ± 18.8 mins (Benoit et al., 1980) vs 66.7 ± 14.4 mins (Aeschbach et al., 1996)) although there was overlap within their standard deviations. Taken together, these studies characterize baseline sleep and various aspects of sleep-wake behavior during recovery from sleep deprivations of 8, 20, and 24 h from usual sleep onset.

Sleep duration and timing are controlled by interactions between circadian propensity for sleep and homeostatic regulation of sleep need that increases with time awake. Homeostatic regulation is likely composed of multiple physiological substrates including adenosine, prostaglandin, and neuronal nitric oxide synthase (Basheer et al., 2004; Huang et al., 2007; Morairty et al., 2013). Slow wave activity (SWA) in the EEG has been correlated with sleep need, and studies measuring SWA under different conditions have provided many of our current insights into the dynamics of the homeostatic sleep drive. Based on these dynamics, mathematical models typically describe the homeostatic sleep drive as a single variable with exponential growth and decay (Daan et al., 1984; Phillips and Robinson, 2007; Diniz Behn et al., 2007; Diniz Behn and Booth, 2010; Booth and Diniz Behn, 2014; Gleit et al., 2013; Rempe et al., 2010; Kumar et al., 2012).

Interestingly, measures of SWA dynamics in habitual short sleepers and habitual long sleepers suggest that the time constants of the growth and decay of homeostatic sleep drive are similar between sleeper types (Aeschbach et al., 1996). Similarly, in an experiment where the time constant for the increase of the homeostatic sleep drive was estimated from wake EEG, no difference between habitual short and long sleepers was found (Aeschbach et al., 2001). Instead, it has been suggested that differential responses to sleep deprivation between short and long sleepers result from differences in the tolerance for homeostatic sleep pressure (Aeschbach et al., 2001) with short sleepers living under higher homeostatic sleep pressure and experiencing a shorter biological night (e.g., shorter duration of melatonin secretion) compared to long sleepers (Aeschbach et al., 2003).

In this paper, we use computational modeling to investigate this hypothesis regarding differential levels of homeostatic sleep pressure in different habitual sleeper types, and we explore implications of sleeper type on recovery from acute sleep deprivation. We fit a physiologically-based model of sleep-wake regulation to data of baseline sleep behavior from long, regular, and short sleep-

ers to construct populations of individual sleepers of each type. We validated the sleep deprivation responses of the modeled populations with data on recovery sleep from acute sleep deprivation experiments (Benoit et al., 1980; Aeschbach et al., 1996). We then applied the model to predict differences between sleeper types in response to acute sleep deprivations for a wide range of durations. Model results predict that sleeper types display similar trends in first recovery sleep episodes, however, they demonstrate some key differences in response to some specific sleep deprivation challenges and in the durations of waking episodes following recovery sleep.

2. Methods

In this section, we review model equations for the sleep-wake regulation network model for human sleep. This model was developed to describe typical human sleep (Gleit et al., 2013), but here we construct distinct ensembles of parameter sets to simulate experimental data on sleep behavior for long, regular and short sleepers. We additionally extend the model to include external wake-promoting inputs for simulation of sleep deprivation.

2.1. Model equations

2.1.1. Wake, REM, NREM, and SCN neuronal populations

The sleep-wake regulatory network model introduced in Gleit et al. (2013) is based on current hypotheses for the interactions of hypothalamic and brainstem neural populations that influence behavioral state. A schematic of the model summarizes the modeled connectivity among neuronal populations that have been identified to promote wake (W), NREM sleep (NREM), and REM sleep (REM) states, a suprachiasmatic nucleus population (SCN) that propagates the intrinsic circadian rhythm (C) to the other neuronal populations, and the homeostatic sleep drive variable (H) which modulates activity of the NREM population (Fig. 1A). Synaptic interactions among the populations are mediated by neurotransmitter concentrations expressed by the populations. In the model, the wake population represents the joint activity of the LC and dorsal raphe and their neurotransmitters norepinephrine and serotonin (represented by NE); the NREM population represents the ventrolateral preoptic nucleus and its gammaaminobutyric acid (GABA)-mediated signalling; and the REM population represents the cholinergic REM-on areas of the LDT and PPT. For simplicity, we model the multi-synaptic pathway from the SCN to the sleep-wake regulatory populations as direct projections with the net effect of SCN signalling acting to promote waking and suppress sleep consistent with SCN activity profiles and human sleep-wake behavior. Thus, while we refer to the SCN neurotransmitter as GABA, since it is the primary neurotransmitter in SCN neurons, the net influence of SCN signaling on sleep- and wake-promoting populations may be mediated by other neurotransmitters/neuromodulators. For more details of the model, we refer the reader to Gleit et al. (2013).

In our model formalism, we assume that the mean firing rate (in Hz) of a presynaptic neuronal population, $F_Y(t)$ (Y = Wake, NREM, REM and SCN) drives the release of neurotransmitter at the postsynaptic population to affect its firing rate $F_X(t)$ (X = Wake, NREM and REM). Thus, the rate of change of F_X is given by:

$$\frac{dF_X}{dt} = \frac{F_{X\infty}\left(\sum_i g_{iX} R_{i\infty}(F_Y)\right) - F_X}{\tau_X},\tag{2.1}$$

where $F_{X\infty}$ is the firing rate response function, g_{iX} is a nondimensional weight parameter, $R_{i\infty}$ is the neurotransmitter release function, and τ_X is the time scale at which $F_X(t)$ evolves. Whether a connection between populations X and Y is inhibitory or

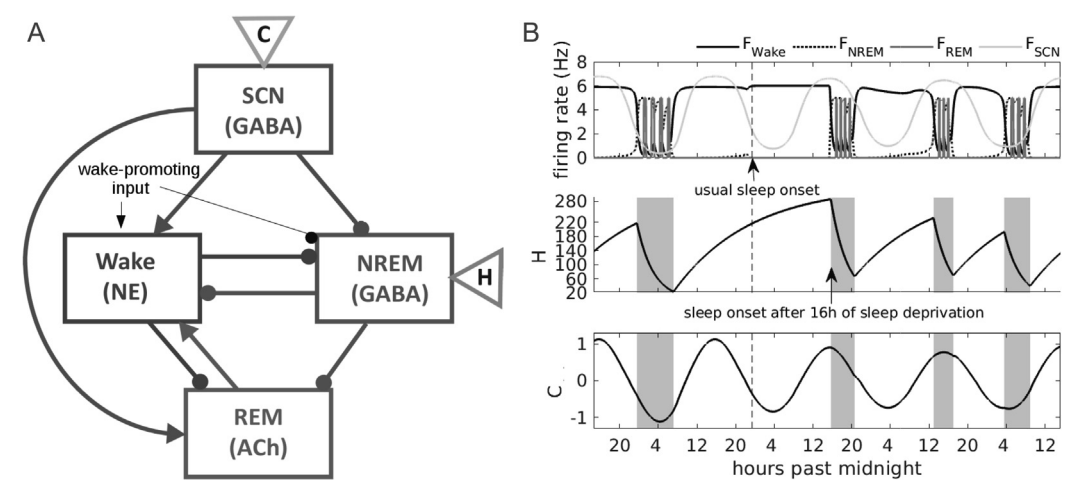


Fig. 1. Model schematic and simulation results for 16 h of sleep deprivation. A. Model schematic indicating neuronal populations (i.e., Wake, SCN, NREM, and REM), their respective neurotransmitters (NE, GABA, and ACh), and the sites of action of the homeostatic sleep variable (H) and the circadian drive (C) included in the human sleep-wake regulatory network model (Gleit et al., 2013). Projections among neuronal populations are denoted with arrows when excitatory and circles when inhibitory. Wake-promoting inputs associated with simulating sleep deprivation affect both the Wake and NREM populations. Full equations describing the time evolution of the average firing rate of each neuron population are provided in the Supplemental Material. B. Numerical simulation results of the sleep-wake network model with parameter values for a regular sleeper during a 16 h sleep deprivation and the immediate recovery period. (The three panels share the x-axis, see vertical ticks in each subpanel.) (Top panel) Average firing rates of the Wake, NREM, REM, and SCN populations with arrow and dashed vertical line indicating the timing of usual sleep onset; (middle panel) the homeostatic sleep drive variable H(t) with arrow indicating the time of sleep onset after 16 h of sleep deprivation; and (bottom panel) the circadian drive variable C(t). Sleep and wake episodes are indicated with a gray or white background, respectively.

excitatory depends on the sign of the weight g: For g>0 (g<0), the neurotransmitter released by neuronal population Y excites (inhibits) X. Thus, the function $F_{X\infty}$ takes a weighted sum of neurotransmitter concentrations $R_{i\infty}$ (released because of the activity in presynaptic neuronal population Y) as its argument. This function has a sigmoidal form which saturates for high levels of total input r as follows:

$$F_{X\infty}(r) = \frac{X_{\text{max}}}{2}(1 + \tanh((r - \beta_X)/\alpha_X)), \tag{2.2}$$

where X_{\max} is the maximum firing rate, β_X is the half-activation threshold, and α_X is the sensitivity of the response of population X. The neurotransmitter concentration released as a result of the activity in the presynaptic neuronal population depends on the mean firing rate of the presynaptic neuronal population F_Y . This dependency is determined by the steady state neurotransmitter release function, $R_{i\infty}$ (i = NE, GABA, ACh and S (for SCN released neurotransmitter)), for a presynaptic firing rate f as follows:

$$R_{i\infty}(f) = \tanh(f/\gamma_i), \tag{2.3}$$

where γ_i is the sensitivity of the release. In the reduced version of the model, we make the simplifying assumption of instantaneous neurotransmitter release by the presynaptic neuronal population, that is, $F_X' \ll R_i'$. This simplification reduces the dimensionality of the model, and based on numerical simulations, does not qualitatively affect model dynamics. For the model equations describing the time evolution of the firing rates F_{Wake} , F_{REM} , F_{NREM} , and F_{SCN} and a listing of model parameter values, see Supplemental Material.

2.1.2. Circadian oscillator model

Twenty-four hour variation in the SCN population firing rate, F_{SCN} , is driven by the human circadian clock model previously introduced in (Forger et al., 1999; Serkh and Forger, 2014) and based on a modified version of the Van der Pol oscillator. Its primary output variable C(t) replicates the 24-h rhythm observed in human circadian markers, such as the body temperature, and its response to external light input has been fit to human data (Forger et al., 1999; Kronauer et al., 1999). The dynamics of C(t) and a complementary variable, x_C , are governed by:

$$\frac{dC}{dt} = \left(\frac{\pi}{12}\right)(x_C + B) \tag{2.4}$$

$$\frac{dx_{C}}{dt} = \left(\frac{\pi}{12}\right) \left[\mu \left(x_{C} - \frac{4x_{C}^{3}}{3}\right) - C\left(\left(\frac{24}{0.99669\tau_{x}}\right)^{2} + kB\right) \right], \tag{2.5}$$

where $\mu=0.23$ represents the stiffness of the oscillator, $\tau_x=24.2$ h is the period of the oscillator, and k=0.55 modulates the effect of the light input B. We follow (Forger et al., 1999) and incorporate a circadian sensitivity modulation to external light input

$$B = \widehat{B}(1 - 0.4C)(1 - 0.4x_C), \tag{2.6}$$

with

$$\widehat{B} = G(1 - n)\alpha(I), \tag{2.7}$$

where G = 33.75 and variables n and α govern the external light intensity I as follows:

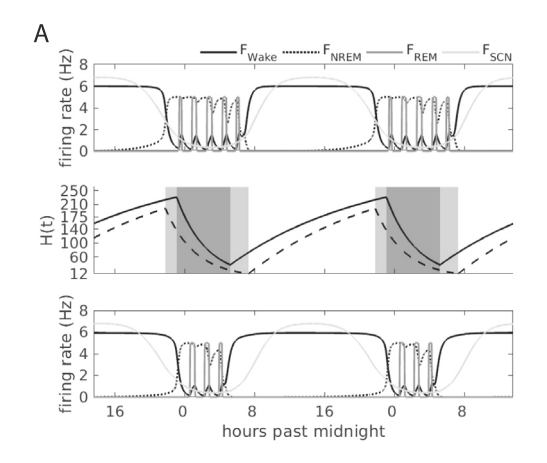
$$\alpha(I) = \alpha_0 \left(\frac{I}{I_0}\right)^p,\tag{2.8}$$

$$\frac{dn}{dt} = 60(\alpha(I)(1-n) - \beta n),\tag{2.9}$$

where $I_0=9500$ lux, $\alpha_0=0.05 {\rm min}^{-1}$, p=0.5, and $\beta=0.0075 {\rm min}^{-1}$. This circadian model generates oscillations in C between -1 and 1 that can be entrained to a 24-h light:dark schedule given by I(t). This drives oscillations in the average firing rate of the SCN population, F_{SCN} , between 1 and 7 Hz which is in agreement with experimental data on the neuronal activity in SCN in mammals (Deboer et al., 2003). For the light schedule, we simulate an 14-h:10-h environmental light:dark cycle with light intensity 5000:0 lux. Actual light input to the circadian model is gated by sleep-wake behavior such that if the model is awake during the dark period, light intensity is 500 lux and if the model is asleep during the light period, light intensity is 100 lux.

2.1.3. The homeostatic sleep drive H

Activity of the NREM population is influenced by the homeostatic sleep drive, H, which represents the power of slow wave activity (SWA) (i.e., electroencephalogram (EEG) power in the



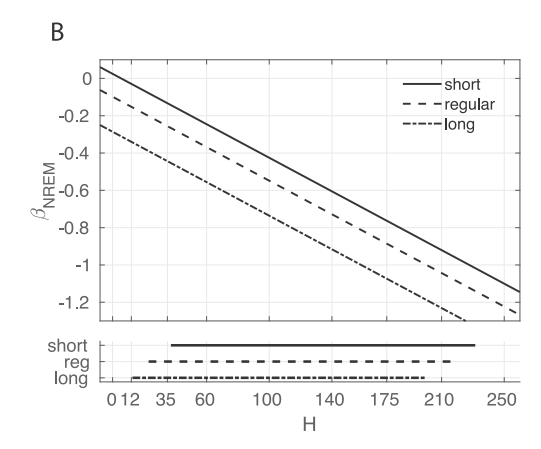


Fig. 2. Simulating habitual long and short sleepers. A. Numerical simulation of habitual long (top panel) and short (bottom panel) sleepers. The sleep homeostat H for each sleeper type (middle panel) attains higher homeostat values for short sleepers (solid line) compared to long sleepers (dashed line). B. The homeostatic sleep drive acts by modulating the half-activation threshold, $β_{\text{NREM}}(H)$ of the NREM response function $F_{\text{NREM}\infty}$ as a function of H. Different sleeper types are simulated by varying the parameter $b_{H\beta}$ in the half-activation threshold: $β_{\text{NREM}}(H) = -0.0045H + b_{H\beta}$, thereby changing the H dependence (top panel). This affects the H values associated with sleep and wake onsets for each sleeper type (bottom panel).

range between 0.75 and 4.5 Hz) during slow wave sleep in humans (see, e.g., (Rusterholz et al., 2010). The dynamics of *H* are given by the following equation

$$\frac{dH}{dt} = \frac{(H_{\text{max}} - H)}{\tau_{\text{Hw}}} \mathcal{H}[F_W - \theta_W] - \frac{H}{\tau_{\text{Hs}}} \mathcal{H}[\theta_W - F_W], \tag{2.10}$$

where \mathscr{H} is a Heaviside function, $^{1}H_{\text{max}}$ is the maximum % of the mean SWA, and au_{Hw} and au_{Hs} are the time constants for the exponential increase during wake and decrease during sleep in the power of the SWA, respectively. Our choice of values for these three parameters is based on experimental results of EEG recordings in humans done by Rusterholz et al. (2010). We assume that the state of decrease (sleep) or increase (wake) of the homeostatic sleep drive is governed by the mean firing rate of the wake population. That is, the homeostatic sleep drive starts to increase (decrease) (and the model is in wake (sleep) state) when F_{Wake} crosses its threshold value θ_W from below (above). H influences the transitions between wake and sleep states through its modulation of the excitability of the NREM population. Specifically, H varies the half-activation threshold of the NREM population response function $F_{NREM\infty}$ as follows: $\beta_{NREM}(H) = -0.0045H + b_{H\beta}$. In this way, high (low) values of H promote activation (deactivation) of the NREM promoting population.

2.2. Simulating sleep deprivation

In numerical simulations of the sleep-wake model, behavioral states are determined by the neuronal populations that have the highest firing rates, with REM sleep occurring when both F_{REM} and F_{NREM} are high (Fig. 1B). To simulate sleep deprivation, an additional external input is applied to the wake and NREM populations (Fig. 1A) that increases the activity of F_{Wake} and inhibits that of F_{NREM} . Biologically, such an input can be considered as a process or effect of behavior that promotes waking and suppresses sleep beyond the time when sleep would occur under normal conditions. Wake-promoting behaviors, which may involve dopamine or orexin signaling, or consumption of caffeine near the usual bed time are examples of such processes. In the model, we represent the wake-promoting (sleep-suppressing) input as an additional constant input (of value 10) that increases (decreases) the total input to the Wake (NREM) population starting an hour before the

usual sleep onset (as occurs around 23 h of the 2nd day in Fig. 1B). We denote the number of hours (beyond the usual sleep onset) when this additional input is active as $t_{\rm sd}$, and we consider $1 \le t_{\rm sd} \le 24$.

As described above, we fix the light level to be I = 500 lux if the model is in the wake state during the dark period of the light:dark cycle. This mimics a more realistic light environment during sleep deprivation in experimental settings in which the participants were engaged in watching movies or studying during their sleep-deprivation period (Aeschbach et al., 1996).

2.3. Constructing model populations for different sleeper types

We represented long, regular, and short sleepers by varying the levels of homeostatic sleep pressure at which sleep-wake transitions occur, with short sleepers exhibiting the highest sleep pressures. In our model, values of the homeostatic sleep drive H at sleep-wake transitions are determined by the H-modulation of the NREM population activation response. Specifically, H values associated with state transitions are governed by the halfactivation threshold, $\beta_{\text{NREM}}(H)$, of the NREM response function $F_{\text{NREM}\infty}$ where $\beta_{\text{NREM}}(H) = -0.0045H + b_{H\beta}$. By varying the baseline half-activation threshold, $b_{H\beta}$, simulated sleep durations and ranges of H values varied as predicted by sleeper type (Fig. 2). In particular, low or high values of $b_{H\beta}$ varied the sensitivity of the NREM population to increases in H and thus produced simulated sleep-wake episodes with longer or shorter sleep periods, respectively, and lower or higher ranges of H values, respectively (Fig. 2A).

To optimize model parameters to replicate experimentally reported sleep-wake patterns of the three sleeper types, we took a model population approach. For each sleeper type, we constructed an ensemble of $\sim 20,000$ parameter sets that yielded statistically equivalent fits to experimental measurements of the baseline sleep-wake behavior in habitual long, regular, and short sleepers (Aeschbach et al., 1996; Benoit et al., 1980). Model ensembles were constructed using a Markov chain Monte Carlo algorithm (Chib and Greenberg, 1995), implemented in Sloppycell (Myers et al., 2007 (sourceforge.net/p/sloppycell)), by varying $b_{H\beta}$ and five weight parameters (i.e., $g_{S,Wake}, g_{S,NREM}, g_{GABA,Wake}, g_{NE,REM}$ and $g_{GABA,REM}$). Through parameter sensitivity analysis, these parameters were determined as the minimal set of parameters that exerted independent effects on the timing and durations of sleep

¹ That is, $\mathcal{H}[z] = 0$ if z < 0 and $\mathcal{H}[z] = 1$ if $z \ge 0$.

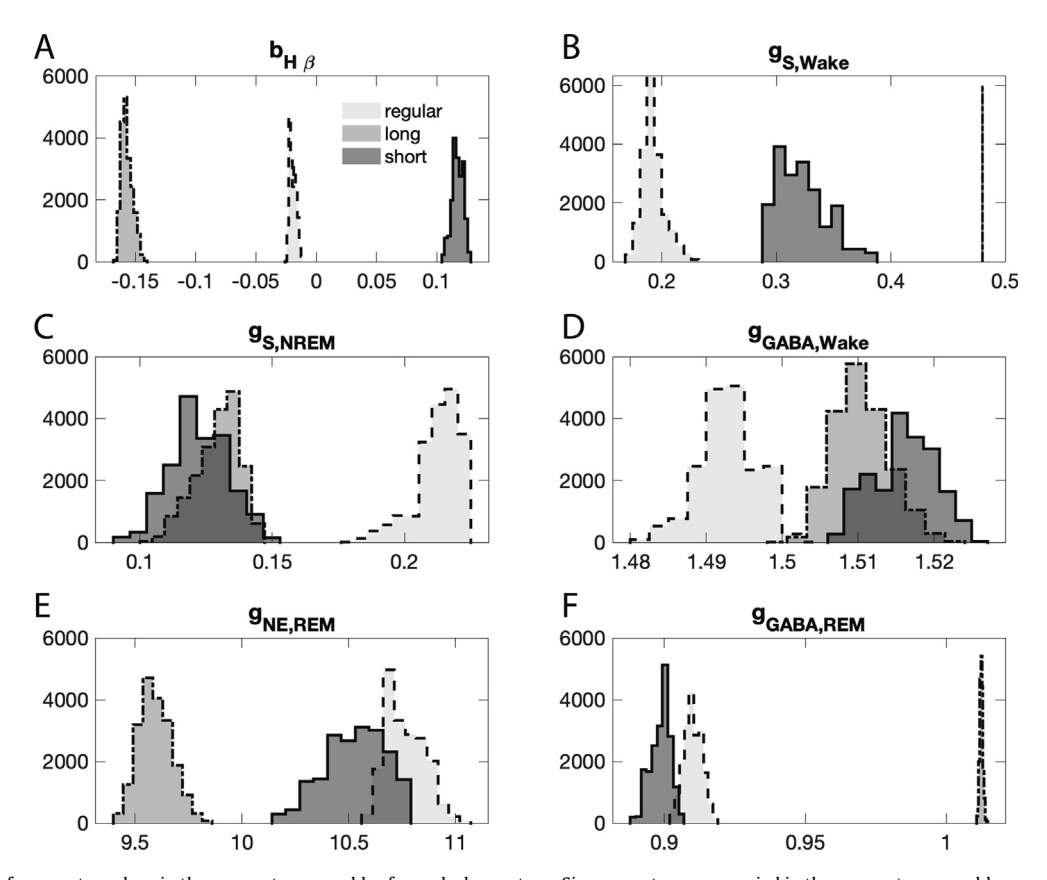


Fig. 3. Distributions of parameter values in the parameter ensembles for each sleeper type. Six parameters were varied in the parameter ensembles representing each sleeper type. A. The baseline activation threshold of the NREM-promoting neuronal population, $b_{H\beta}$ was the key parameter affecting sleep duration and showed distinct parameter ranges for each sleeper type. B.–F. Parameters governing the strengths of interactions between populations also contributed to the fitting for each sleeper type. In particular, we varied projections from the SCN to the wake- and NREM-promoting populations, $g_{S,Wake}$ (B) and $g_{S,NREM}$ (C), respectively; from the NREM- to wake-promoting populations, $g_{GABA,Wake}$ (D); and from the wake- and NREM-promoting populations to the REM-promoting population $g_{NE,REM}$ (E) and $g_{GABA,REM}$ (F) across sleeper types. For the long sleeper parameter ensemble, $g_{S,Wake}$ was not varied due to constraints associated with REM sleep durations during recovery from sleep deprivation (see Section 3.1).

and wake episodes (Fig. 3). Remaining parameters were set to values appropriate for human sleep as previously identified (Gleit et al., 2013; Booth et al., 2017) (see Supplemental Material). We note that other model parameters such as activation thresholds, β_X , of the response functions, $F_{X\infty}$ can have similar effects on sleep timing and duration. However, these changes can be compensated by variation in the weight constants, thus they do not result in independent effects on model solutions.

To capture interindividual variability within sleeper types, we then constructed model populations of 20 individual sleepers of each type by randomly choosing 20 $b_{H\beta}$ values from normal distributions centered at the median $b_{H\beta}$ values of the ensembles, and setting the other varied parameters to their ensemble median values. For these normal distributions, we chose standard deviations of 0.03 in order to capture more variability than is present in the ensemble distributions for $b_{H\beta}$ (Fig. 3). This choice additionally maintained distinct sleeper types as the overlap between groups was limited to the 1% tails of the distributions (see Fig. 4). For model results shown in Figs. 5–7, we simulated the model with the parameter values for the 20 "individuals" of each sleeper type.

3. Results

3.1. Modeling populations of long, regular and short sleepers

In the simulations of the different sleeper groups, we focus on the model parameter $b_{H\beta}$ that significantly affected the mean values of H across the sleep-wake cycle and the duration of sleep episodes (see Section 2.3 and Fig. 2 for details). In particular, we

optimized model parameters, varying the minimal number that had independent effects, to fit experimental measurements of baseline sleep-wake behavior in habitual long, regular and short sleepers (Aeschbach et al., 1996; Benoit et al., 1980) by constructing ensembles of parameter sets that exhibited statistically similar fits (for more details, see Section 2.3). Indeed, the optimized parameter ensembles showed clear separation in $b_{H\beta}$ values for long, regular and short sleepers (Fig. 3).

In general, responses to simulated sleep deprivation were not used to fit model parameters. However, we found that the weight parameter for the influence of the SCN population on the wake-promoting population, $g_{S,Wake}$, strongly affected the amount of REM sleep during recovery sleep from sleep deprivation, but had less effect on REM sleep durations during baseline sleep. Thus, in order to capture the appropriate REM sleep behavior during recovery sleep, this parameter was fixed for the long sleeper parameter ensembles (Fig. 3B).

For each sleeper type, sleep deprivation was simulated for the 20 "individual" sleepers with different $b_{H\beta}$ values (see symbols in Fig. 4) to generate baseline and recovery sleep-wake behavior. Thus, with this model population approach, we accounted for interindividual variability within sleeper types and generated model results appropriate for comparison to experimental data from a cohort of individuals.

3.2. Comparing sleep deprivation simulations with experimental data

We validated our model populations of sleeper types by comparing model simulations and published experimental data on

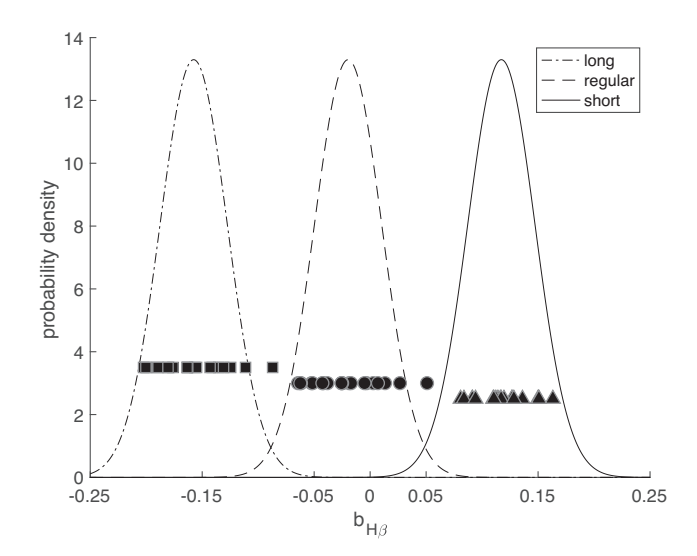


Fig. 4. Interindividual variability in the key parameter $b_{H\beta}$. We accounted for interindividual variability within sleeper types by generating 20 values (symbols) for the parameter $\mathbf{b}_{H\beta}$ from normal distributions (with standard deviation 0.03) centered around the ensemble median value for each sleeper type. These values were used to construct parameter sets representing 20 "individuals" of each sleeper type (all other parameters were fixed to their ensemble median values, to facilitate comparison with experimental data from the three sleeper types (see Figs. 5 and 6).

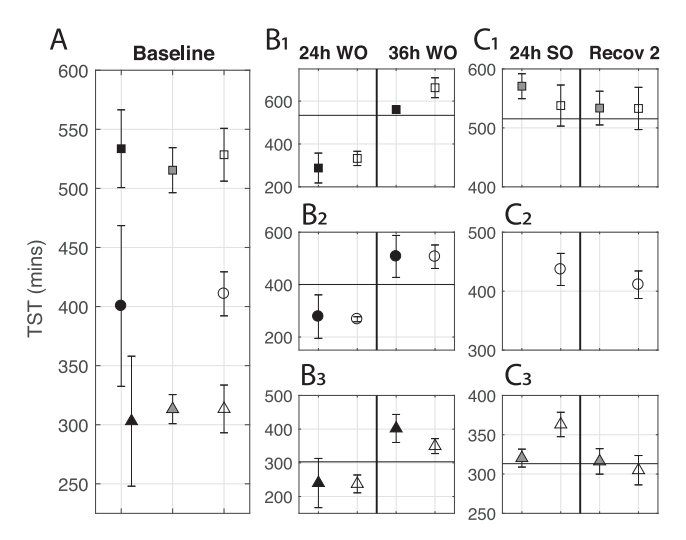


Fig. 5. Experimental data and model simulations for total sleep times (TST) in baseline conditions and in response to acute sleep deprivation for 3 sleeper types. Published experimental data (filled symbols; black symbols representing long, regular, and short sleepers from Benoit et al. (1980); gray symbols representing long and short sleepers from Aeschbach et al. (1996) and model simulation results (open symbols) for long (squares), regular (circles), and short (triangles) sleepers are compared. For each condition, model results show the mean and standard deviation from simulations of 20 "individuals" of each sleeper type. A. Total sleep time (TST) under baseline conditions. B. Recovery sleep after sleep deprivations of 24 (left column) and 36 (right column) h after wake onset for long (B_1) , regular (B_2) , and short (B₃) sleepers. Horizontal lines denote the baseline sleep duration reported in Benoit et al. (1980). C. Recovery sleep after sleep deprivations of 24 h after sleep onset for long (C1) and short sleepers (C3) on the first (left column) and second (right column) recovery nights. Horizontal lines denote the baseline sleep duration reported in Aeschbach et al. (1996). Since this experimental study did not report data for regular sleepers (Aeschbach et al., 1996), only simulation results are shown for regular sleepers in this condition (C2).

baseline sleep and sleep deprivation recovery for habitual long, regular and short sleepers (Aeschbach et al., 1996; Benoit et al., 1980) (Figs. 5 and 6). Model results for the 20 simulated individu-

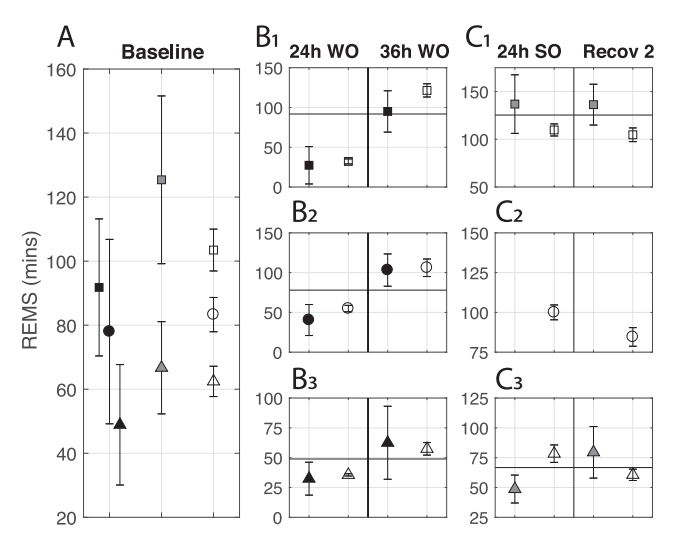


Fig. 6. Experimental data and model simulations for REM sleep (REMS) times in baseline conditions and in response to acute sleep deprivation for 3 sleeper types. Published experimental data (filled symbols; black symbols representing long, regular, and short sleepers from Benoit et al. (1980); gray symbols representing long and short sleepers only from Aeschbach et al. (1996) and model simulation results (open symbols) for long (squares), regular (circles), and short (triangles) sleepers are compared. For each condition, model results show the mean and standard deviation from simulations of 20 "individuals" of each sleeper type. A. REMS time under baseline conditions. B. REMS time during recovery sleep after sleep deprivation of 24 (left column) h and after 36 h (right column) after wake onset for long (B₁), regular (B₂), and short (B₃) sleepers. Horizontal lines denote the baseline REM sleep duration reported in Benoit et al. (1980). C. REMS time during recovery sleep after sleep deprivations of 24 h from sleep onset for long sleepers (C₁) and short sleepers (C₃) on the first (left column) and second (right column) recovery nights. Horizontal lines denote the baseline REM sleep duration reported in Aeschbach et al. (1996). This experimental study did not report data for regular sleepers (Aeschbach et al., 1996) so only model results are shown (C2).

als fell in the ranges of variability of the experimental data for each sleeper type. Specifically, for total sleep times, our model simulations for all three sleeper types were within the standard deviations of both data sets (Fig. 5). For REM sleep time, there was more variability between published experimental results, but model results were within the overlap ranges of the standard deviations of the data sets (Fig. 6).

We validated our model by comparing the total and REM sleep durations after acute sleep deprivation with the experimental data for the three reported deprivation durations. Namely, when recovery sleep occurs i) 24 or ii) 36 h after wake onset (Benoit et al., 1980) (Figs. 5B₁-B₃ and 6B₁-B₃), or iii) 24 h after previous sleep onset (Aeschbach et al., 1996) (Figs. 5C₁-C₃ and 6C₁-C₃). Model simulations of the three sleep deprivation protocols generally replicated, both qualitatively and quantitatively, total recovery sleep durations for each sleeper type (Fig. 5). The length of recovery sleep predicted by the model fell within the error margins reported in the data, with two exceptions: 1) overestimation of the long sleepers' recovery sleep when recovery sleep was initiated 36 h after previous wake onset (Fig. 5B₁, right) and 2) overestimation of the short sleepers' recovery sleep after 24 h of sleep deprivation (Fig. 5C₃, left).

Similarly, model simulations of REM sleep durations during recovery sleep showed good agreement, both qualitatively and quantitatively, with REM sleep data across the three sleeper types (Fig. 6). Specifically, model results reproduced trends or fell within the error margins of the data, except for an underestimation of REM sleep duration for the long sleepers' second recovery night (Fig. 6C₁, right) and an overestimation of short sleepers' recovery after 24 h of sleep deprivation (Fig. 6C₃, left).

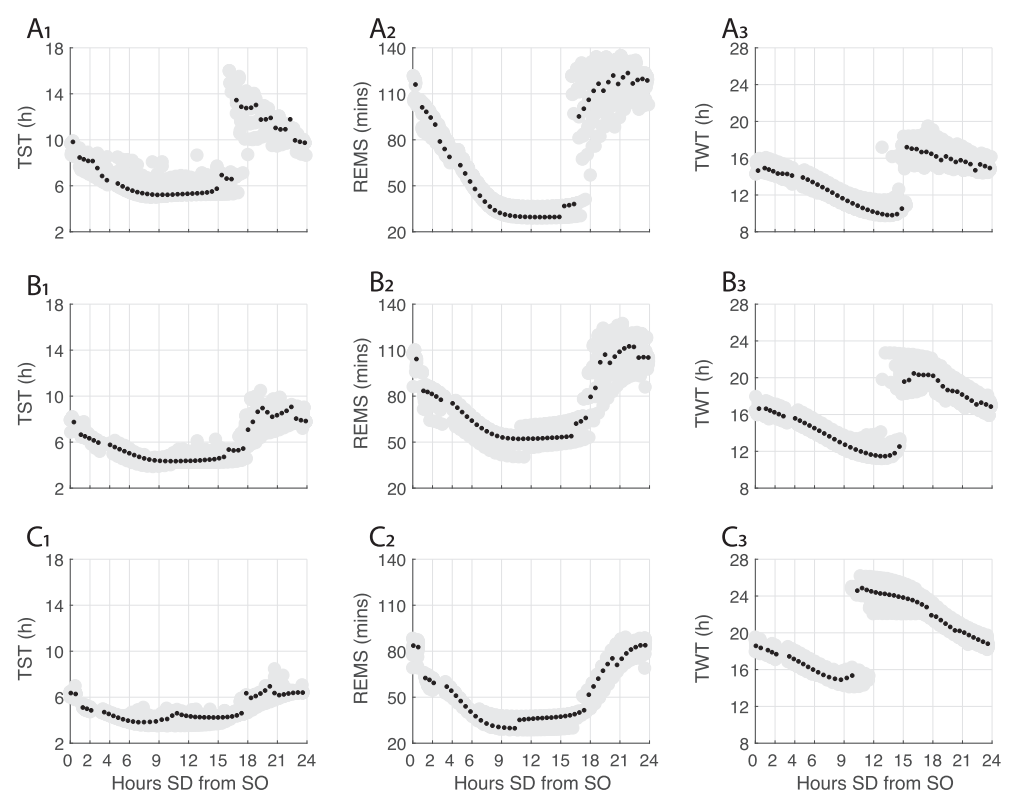


Fig. 7. Predicted sleep, REM sleep, and wake times during recovery from 0–24 h of sleep deprivation for 3 sleeper types. Simulated durations of total sleep time (TST) during recovery sleep (A₁, B₁, and C₁); REM sleep time (REMS) during recovery sleep (A₂, B₂, and C₂); and wake time following recovery sleep (TWT) (A₃, B₃, and C₃) for 0–24 h of sleep deprivation (x-axis) for simulated populations of long (**A**), regular (**B**), and short (**C**) sleepers. TST, REMS, and TWT are represented with respect to the hours of sleep deprivation from typical sleep onsets. Black dots indicate TST, REMS, and TWT durations computed for the ensemble median parameter values for each type; gray dots indicate TST, REMS, and TWT computed for each of the 20 "individuals" in each population and represent interindividual variability within each group.

The experimental data and model results showed strong trends that have been previously reported for durations of recovery sleep following sleep deprivation. In particular, recovery sleep was shorter than baseline sleep when sleep was delayed until 24 h after wake onset but longer than baseline sleep if sleep was allowed 36 h after wake onset. This phenomenon occurred for both total and REM sleep durations and in both experimental data and model simulations, across all three sleeper types. These cases correspond to sleep deprivation of 8 and 20 h, respectively, after usual sleep onset, and a similar pattern has been observed previously in both human data (Akerstedt and Gillberg, 1981) and modeling studies (Rempe et al., 2010; Kumar et al., 2012; Phillips and Robinson, 2008) (see Discussion).

3.3. Predicted recovery sleep and subsequent wake durations

While the experiments only reported recovery from a few sleep deprivation durations, using the model we predicted the length of recovery sleep and subsequent wake for sleep deprivations of 0 to 24 h from usual sleep onset for the simulated populations of long, regular, and short sleepers. Durations of recovery TST, recovery REM sleep, and total wake time (TWT) following recovery sleep are represented with respect to the number of hours of sleep deprivation from typical sleep onset (Fig. 7). Both simulated results for the ensemble median parameter values and "interindividual" variability within the simulated populations are presented. All sleeper types had shorter recovery TST and REM sleep durations, relative to baseline, for sleep deprivations less than approximately 17 h when recovery sleep would be occurring when circadian drive for wakefulness was high. For all sleeper types, the shortest recovery sleep (approximately 4–5 h) occurs when sleep onset takes place

between 6 and 15 h after the usual sleep onset. There was also significant variability in REM sleep during recovery sleep among sleeper types. Although the shortest REM sleep duration occurred following 9–15 h of sleep deprivation for all types, regular sleepers had longer REM sleep times compared to other types, and long sleepers had much less REM sleep relative to baseline durations compared to other types. These findings were consistent with experimental results (see Discussion) (Benoit et al., 1980).

For between 16 and 18 h of sleep deprivation, recovery TST and REM sleep durations started to increase with long and regular sleepers showing a sharp increase or jump in durations. These increases in recovery sleep correspond to sleep onset occurring during the waning phase of the circadian rhythm and sleep episodes continuing through the circadian phases when sleep usually occurred. Interindividual variability in TST and REM sleep durations was greatest around these jumps for long and regular sleepers, with "individuals" exhibiting different numbers of REM sleep episodes. Long sleepers showed the largest jumps in recovery TST and REM sleep with the longest rebound sleep durations above baseline sleep duration. On the other hand, short sleepers displayed reduced variability in TST and REM sleep durations.

TWT following recovery sleep also showed similar qualitative changes for all sleeper types with wake periods shorter than baseline wake periods for sleep deprivations up to 12–15 h and a sharp increase in TWT, that was longer than baseline wake periods for regular and short sleepers, for longer sleep deprivations. However, the jump to longer wake periods occurred with shorter amounts of sleep deprivation (~9–12h) for short sleepers compared to the other types. Short sleepers also showed longer recovery wake periods compared to other types across the range of sleep deprivation durations with up to 24 h of wake predicted for short sleepers

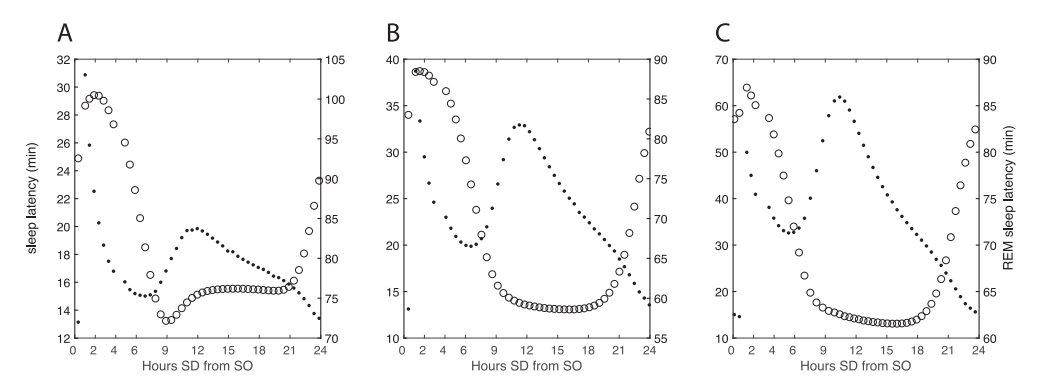


Fig. 8. Predicted latencies to sleep and to REM sleep following 0–24 h of sleep deprivation for 3 sleeper types. Latency to sleep (dots, left vertical axis) and to REM sleep (open circles, right vertical axis) was computed from simulated sleep deprivations of 0–24 h from sleep onset for long (A), regular (B) and short (C) sleepers as represented by the ensemble median parameters for each sleeper type.

following sleep deprivation of 12 h with a recovery sleep of less than ~ 4 h. By contrast, both regular and long sleepers were predicted to have wake times less than 12 h following a similar schedule of 12 h sleep deprivation and less than 6 h recovery sleep. These differences in resilience to short recovery sleep are consequences of the differences in levels of homeostatic sleep drive among the three sleeper types (see Discussion).

Latencies to sleep and to REM sleep during recovery sleep episodes also were affected by the amount of sleep deprivation (Fig. 8). We defined sleep latency as the difference in time between when the external wake-promoting input ended (i.e., t_{sd} , see Section 2.2) and the time of sleep onset. We defined REM sleep latency as the difference in time between the start of the first REM bout and sleep onset. All sleeper types showed longer sleep and REM latencies compared to baseline for 1-2 h of sleep deprivation, but latencies then decreased as the number of sleep deprivation hours increased. This is expected due to increases in homeostatic sleep drive with delayed sleep onset. However, sleep latency then increased for ~8-12 h of deprivation coinciding with sleep onset occurring when circadian drive for wakefulness was highest. REM sleep latency, on the other hand, remained low for all sleeper types without showing a circadian effect. Long sleepers showed the shortest sleep latencies, but the longest REM latencies compared to other sleeper types.

3.4. Predicted return to baseline sleep behavior

It has been suggested that full recovery from acute sleep deprivation typically requires 1–3 nights of usual sleep (Bonnet, 2000). To assess the time course of recovery to baseline behavior over multiple days, we simulated recovery sleep and wake behavior for 5 days following the acute sleep deprivation. For most durations of sleep deprivations, our model simulations showed recovery within 3 nights, however, there were some differences among sleeper types (Fig. 9). For simulated long and regular sleepers, TST and REM sleep of recovery sleep, and TWT following recovery sleep return to baseline durations by the third recovery episode for almost all hours of sleep deprivation. However, both of these sleeper types showed long-lasting effects for 16-17 h of sleep deprivation such that durations of sleep, REM and wake episodes did not return to baseline by the 5th recovery episode. Interestingly, these hours of sleep deprivation coincided with the jump in recovery TST and REM sleep, and thus represent the border between sleep deprivation regimes that produce initial recovery sleep periods that are shorter than baseline sleep durations from those that are longer than baseline sleep durations. The convergence back to baseline behavior following the first recovery sleep episode differed between these two regimes with successive sleep durations lengthening for sleep deprivations less than 16 h and shortening for sleep deprivations greater than 17 h. The slower convergence back to baseline behavior for sleep deprivation between 16–17 h suggests a more complicated recovery pattern that may include shorter and longer than baseline sleep durations. By contrast, simulated short sleepers achieved full recovery to baseline by the fifth recovery episode for all sleep deprivation hours. However, short sleepers also showed slower recovery for certain sleep deprivation durations with TST, REM, and wake episodes above baseline levels at the 3rd recovery episode for sleep deprivations of 10–15 h.

4. Discussion

In this work, we applied a physiologically-based mathematical model to investigate the responses to acute sleep deprivation in simulated populations of habitual long, regular and short sleepers with a focus on effects of differences in homeostatic sleep drive levels among sleeper types. After fitting the model to experimental data of baseline sleep behavior in different sleeper types, model results accurately replicated responses to data from specific sleep deprivation protocols (see Benoit et al., 1980; Aeschbach et al., 1996) and general trends in sleep deprivation responses that have been reported in experimental and modeling studies (Akerstedt and Gillberg, 1981; Daan et al., 1984). Model results predicted the responses of long, regular, and short sleepers to 0–24 h of acute sleep deprivation and provided insight into differences in recovery sleep across sleeper types.

In general, we found that the relative contributions of circadian and homeostatic effects on sleep varied with the timing of recovery sleep. Since modeled homeostatic, but not circadian, effects depended on sleeper type, the sleeper type-dependent differences in recovery sleep also varied with the timing of recovery sleep. For example, the short recovery sleep durations that occurred during morning hours (following 6-15 h of sleep deprivation) is primarily dictated by the strong circadian waking drive at these times and was similar for all sleeper types. This suggests that differences in homeostatic sleep drive have little effect on recovery sleep at these times, consistent with experimental measurements showing that recovery sleep was essentially the same duration for all sleeper types after 24 h of sleep deprivation from previous wake onset (equivalent to approximately 6-9 h of sleep deprivation from habitual sleep onset) (Benoit et al., 1980). By contrast, after approximately 16 h of sleep deprivation, all sleeper types showed a sudden increase in recovery sleep duration for sleep onsets of 12 to 18 h past habitual bedtime with longer and more variable sleep durations in simulated long and regular sleepers. These results, including high inter-individual variability in timing and magnitude

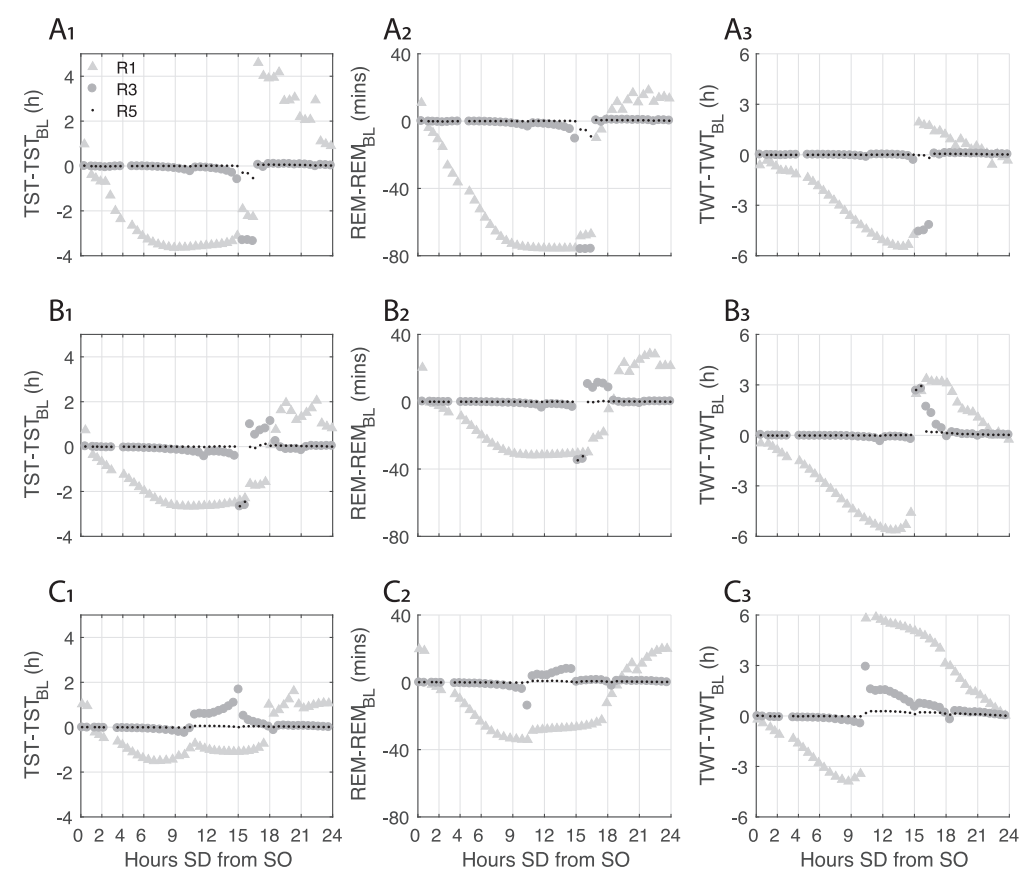


Fig. 9. Predicted time course for recovery to baseline behavior following acute sleep deprivation for 3 sleeper types. Model results for the differences between behavior during recovery following 0–24 h of sleep deprivation and baseline behavior during the first (R1, triangles), third (R3, circles), and fifth (R5, dots) recovery episodes for long (A), regular (B) and short (C) sleeper types. Differences are shown between total sleep time (TST) in recovery sleep and baseline TST (TST_{BL}) (first column), between REM sleep time and baseline REM (REM_{BL}) (second column); and between total wake time (TWT) and baseline TWT (TWT_{BL}) (third column). Durations are presented for the ensemble median parameters for each sleeper type and reported as a function of the sleep deprivation (SD) hours relative to the baseline sleep onset time.

of simulated recovery sleep, are consistent with experimental data (Akerstedt and Gillberg, 1981) and suggest that homeostatic sleep drive has a stronger effect on recovery sleep duration at these times.

Furthermore, our simulations predicted interactions between overall recovery sleep and the recovery of REM sleep. It is well documented that the propensity for REM sleep is modulated by the circadian rhythm with the lowest propensity occurring when the circadian waking drive peaks (Czeisler et al., 1980; Sat Bir et al., 2002). Model results replicated this effect with the lowest amount of REM sleep observed in recovery sleep during morning hours (after 9–15 h of sleep deprivation). For sleep deprivations longer than 16 h, a lower circadian waking drive allowed more REM sleep to occur and contributed to the variability of recovery sleep durations across sleeper types with different numbers of REM episodes occurring across the simulated populations of long and regular sleepers.

Interestingly, REM sleep durations in simulated recovery sleep for both short and long sleepers were shorter compared to those for regular sleepers. In addition, model results indicated that long sleepers showed the shortest latencies to sleep but the longest latencies to REM sleep during recovery sleep. A reduction in REM sleep during recovery for long sleepers has been reported in experimental studies, particularly when recovery sleep occurred in the morning (Benoit et al., 1980). This may reflect the competitive recovery of NREM and REM sleep. There is evidence that NREM sleep need is fulfilled before REM sleep need during recovery sleep following sleep deprivation (Carskadon et al., 2011), and experimental data for

different sleeper types indicate that long sleepers may be particularly susceptible to differences in rates of REM and NREM recovery sleep (Aeschbach et al., 1996; Benoit et al., 1980).

In addition, our simulation results indicated that the duration of waking episodes following recovery sleep reflects the different habitual levels of homeostatic sleep drive across sleeper types. Specifically, simulated short sleepers showed much longer subsequent wake durations than simulated regular and long sleepers. Although the homeostatic sleep drive H was highest for the short sleepers after sleep deprivation, it decayed quickly during recovery sleep due to its exponential behavior. Since simulated short sleepers habitually experienced higher levels of homeostatic sleep drive, they were able to maintain long periods of wakefulness after shorter recovery sleep.

Simulated short sleepers also showed faster returns to baseline sleep behavior compared to other groups. While experiments suggest that recovery from sleep loss typically occurs within 1 to 3 nights (Bonnet, 2000), model results predicted longer lasting effects of sleep loss for certain lengths of sleep deprivation and sleeper types. For example, for 16–17 h of sleep deprivation, neither the regular nor the long sleeper types had converged back to their baseline sleep or REM sleep durations by the fifth recovery sleep episode. These sleep deprivation durations were associated with a transition in which the first recovery sleep went from shorter to longer than the baseline sleep duration. The recovery response might be particularly variable in this case due to competing influences of circadian promotion for waking and high homeostatic sleep drive. By contrast, short sleepers returned to baseline

durations by the fifth recovery episode for all durations of deprivations. Furthermore, the range of deprivations associated with long recovery periods was smaller for short sleepers compared to long and regular sleepers. These differences may reflect differences in the circadian phases of sleep onsets among the sleeper types during recovery sleep. In particular, short sleepers' resiliency to high homeostatic sleep drive produced longer recovery wake episodes that allowed subsequent sleep to occur during usual circadian phases, thereby hastening convergence back to baseline sleep behavior.

To explore the hypothesis that differences in habitual levels of homeostatic sleep drive produce differences in sleep-wake behavior and sleep deprivation in long, regular and short sleepers, we used the parameter $b_{H\beta}$ to vary the activation threshold of the NREM-promoting population. We found that the optimized parameter ensembles for the three sleeper types showed clear separation in $b_{H\beta}$ values (i.e., short sleepers were associated with higher $b_{H\beta}$ values which cause higher activation thresholds of the NREMpromoting population) and resulted in different habitual ranges for the homeostatic sleep drive. As a result, short sleepers displayed the highest H values at wake and sleep onsets, and long sleepers the lowest H values. This suggests that habitual short sleepers may be more tolerant of sleep pressure because the activation of NREM sleep-promoting brain areas, such as the VLPO, is less sensitive in these individuals. Physiologically, this difference may reflect lower adenosine receptor density, reduced adenosine release, or other properties of individual neurons or networks. For example, hypocretin (also known as orexin) neurons promote and consolidate sleep through modulation of several neuronal populations represented in our modeled sleep-wake network (Saper et al., 2001; Sakurai, 2007; Adamantidis et al., 2007; Behn et al., 2008; Blumberg et al., 2007). Recent results investigating genetically equivalent fish that display either short or long sleep episodes suggest that increased signaling in the hypocretin system causes habitual short sleep durations (Alié et al., 2018; Jaggard et al., 2018; Leung and Mourrain, 2018). Although we do not explicitly include hypocretin neurons in our model, the action of hypocretin to suppress activation of sleep-promoting neural populations would increase the activation threshold of the NREM-promoting population (b_{HB}) , thereby leading to increased homeostatic sleep drive levels. Other parameters that varied among sleeper types were associated with the strength of projections among neuronal populations in the networks and did not show consistent patterns of differences between the three sleeper types.

Responses to acute sleep deprivation have been modeled previously in the classic Two-Process model of sleep regulation (Daan et al., 1984; Achermann et al., 1993; Mallis et al., 2004; Aeschbach et al., 2001) and in other physiologically-based mathematical models of the sleep-wake regulatory network (Phillips and Robinson, 2008; Kumar et al., 2012; Rempe et al., 2010; Postnova et al., 2018). Additionally, modeling has investigated responses to different types of sleep disruption and restriction such as shift work schedules, forced desynchrony protocols and transmeridian flight travel (Postnova et al., 2012; Postnova et al., 2014; Postnova et al., 2016; Gordon et al., 2018). Predicted durations of recovery sleep in response to acute sleep deprivation in the Two Process Model (Daan et al., 1984) identified the strong qualitative trends that our model results showed, and have been observed in other models (Phillips and Robinson, 2008; Rempe et al., 2010). For example, simulations with the Two Process Model exhibit a jump in recovery sleep durations in response to 16–18 h sleep deprivation past the usual bedtime (Daan et al., 1984). This agrees with our model simulations (see Fig. 7) with recovery sleep durations predicted by the Two Process Model being more consistent with our predictions for long sleepers, rather than regular sleepers (Benoit et al., 1980; Aeschbach et al., 1996). To our knowledge, our model results are the first to consider effects of differing homeostatic sleep drive levels for different sleeper types on durations of recovery sleep and subsequent wake periods.

In this study we showed that long, regular and short sleeper phenotypes can be produced by differential habitual levels of homeostatic sleep drive and demonstrate distinct responses to acute sleep deprivation. Although acute sleep deprivation commonly occurs, many real-world situations involve chronic sleep deprivation with approximately 30% of adult workers in the U. S. population reporting sleep durations less than 6 h (Badr et al., 2015). Such chronic sleep deprivation can seriously impair waking neurobehavioral function (Van Dongen et al., 2003) and has been associated with poor health outcomes including diminished cognitive performance, diabetes, cardiovascular disease, inflammation and increased all-cause mortality risk (Tobaldini et al., 2017; Knutson et al., 2007: Mullington et al., 2009), though these effects may be sensitive to sleeper type. Future work is needed to explore how different sleeper types respond to chronic sleep deprivation and to investigate potential differential vulnerabilities to many of the negative consequences of recurrent short sleep durations based on interindividual differences in sleep need.

CRediT authorship contribution statement

Sofia H. Piltz: Conceptualization, Methodology, Software, Formal analysis, Writing - original draft. **Cecilia G. Diniz Behn:** Conceptualization, Writing - review & editing. **Victoria Booth:** Conceptualization, Methodology, Formal analysis, Writing - review & editing.

Declaration of Competing Interest

The authors declare that they have no known competing financial interests or personal relationships that could have appeared to influence the work reported in this paper.

Acknowledgements

This work was supported by NSF DMS-1853506 (VB, SP) and NSF DMS- 1853511 (CDB).

Appendix A. Supplementary data

Supplementary data associated with this article can be found, in the online version, at https://doi.org/10.1016/j.jtbi.2020.110401.

References

Achermann, P., Dijk, D.-J., Brunner, D.P., Borbély, A.A., 1993. A model of human sleep homeostasis based on eeg slow-wave activity: quantitative comparison of data and simulations. Brain Res. Bull. 31 (1–2), 97–113.

Adamantidis, Antoine R., Zhang, Feng, Aravanis, Alexander M., Deisseroth, Karl, de Lecea, Luis, 2007. Neural substrates of awakening probed with optogenetic control of hypocretin neurons. Nature 450 (7168), 420–424..

Aeschbach, D., Cajochen, C., Landolt, H., Borbely, A.A., 1996. Homeostatic sleep regulation in habitual short sleepers and long sleepers. Am. J. Physiol. – Regulat. Integr. Compar. Physiol. 270 (1), R41–R53.

Aeschbach, D., Postolache, T.T., Sher, L., Matthews, J.R., Jackson, M.A., Wehr, T.A., 2001. Evidence from the waking electroencephalogram that short sleepers live under higher homeostatic sleep pressure than long sleepers. Neuroscience 102 (3) 493–502

Aeschbach, D., Sher, L., Postolache, T.T., Matthews, J.R., Jackson, M.A., Wehr, T.A., 2003. A longer biological night in long sleepers than in short sleepers. J. Clin. Endocrinol. Metabol. 88 (1), 26–30.

Akerstedt, T., Gillberg, M., 1981. The circadian variation of experimentally displaced sleep. Sleep 4 (2), 159–169.

Alié, Alexandre, Devos, Lucie, Torres-Paz, Jorge, Prunier, Lise, Boulet, Fanny, Blin, Maryline, Elipot, Yannick, Retaux, Sylvie, 2018. Developmental evolution of the

- forebrain in cavefish, from natural variations in neuropeptides to behavior. Elife $7\,02$
- Badr, M.S., Belenky, G., Bliwise, D.L., Buxton, O.M., Buysse, D., Dinges, D.F., Gangwisch, J., Grandner, M.A., Kushida, C., Malhotra, R.K., et al., 2015. Recommended amount of sleep for a healthy adult: a joint consensus statement of the american academy of sleep medicine and sleep research society. J. Clin. Sleep Med. 11 (06), 591–592.
- Basheer, R., Strecker, R.E., Thakkar, M.M., McCarley, R.W., 2004. Adenosine and sleep-wake regulation. Prog. Neurobiol. 73, 379–396.
- Benoit, O., Foret, J., Bouard, G., Merle, B., Landau, J., Marc, M.E., 1980. Habitual sleep length and patterns of recovery sleep after 24 hour and 36 hour sleep deprivation. Electroencephal. Clin. Neurophysiol. 50 (5), 477–485.
- Blumberg, Mark S., Coleman, Cassandra M., Johnson, Eric D., Shaw, Cynthia, 2007. Developmental divergence of sleep-wake patterns in orexin knockout and wild-type mice. Eur. J. Neurosci. 25(2), 512–518..
- Bonnet, M., 2000. Sleep deprivation. In: Kyger, M., Roth, T., Dement, W., (Eds.), Principles and Practice of Sleep Medicine, chapter 5, Saunders, Phil., London, pp. 53–71..
- Booth, V., Diniz Behn, C.G., 2014. Physiologically-based modeling of sleep/wake regulatory networks. Math. Biosci. 250, 54–68.
- Booth, V., Xique, I., Diniz Behn, C.G., 2017. One-Dimensional Map for the Circadian Modulation of Sleep in a Sleep-Wake Regulatory Network Model for Human Sleep. SIAM Journal on Applied Dynamical Systems 16 (2), 1089–1112.
- Carskadon, M., Dement, W., 2011. Normal human sleep: an overview. In: Kryger, M., Roth, T., Dement, W. (Eds.), Principles and Practice of Sleep Medicine. Elsevier Saunders
- Chib, S., Greenberg, E., 1995. Understanding the metropolis-hastings algorithm. Am. Stat. 49 (4), 327–335.
- Czeisler, C.A., Zimmerman, J.C., Ronda, J.M., Moore-Ede, M.C., Weitzman, E.D., 1980. Timing of rem sleep is coupled to the circadian rhythm of body temperature in man. Sleep 2 (3), 329–346.
- Daan, S., Beersma, D., Borbely, A., 1984. Timing of human sleep: recovery process gated by a circadian pacemaker. Am. J. Physiol. Reg., Int., Comp. Physiol. 246, R161–R183.
- Dauvilliers, Y., Maret, S., Tafti, Mehdi, 2005. Genetics of normal and pathological sleep in humans. Sleep Med. Rev. 9(2), 91–100..
- Deboer, T., Vansteensel, M., Detarii, L., Meijer, J., 2003. Sleep states alter activity of suprachiasmatic nucleus neurons. Nat. Neurosci. 6, 1086–1090.
- Diniz Behn, C., Booth, V., 2010. Simulating microinjection experiments in a novel model of the rat sleep-wake regulatory network. J. Neurophysiol. 103, 1937–1953.
- Diniz Behn, C., Brown, E.N., Scammell, T.E., Kopell, N.J., 2007. Mathematical model of network dynamics governing mouse sleep–wake behavior. J. Neurophysiol. 97 (6), 3828–3840. PMID:17409167.
- Diniz Behn, C.G., Kopell, N., Brown, E.N., Mochizuki, T., Scammell, T.E., 2008. Delayed orexin signaling consolidates wakefulness and sleep: physiology and modeling. J. Neurophysiol., 99 (6), 3090–3103..
- Van Dongen, Hans P.A., 2006. Shift work and inter-individual differences in sleep and sleepiness. Chronobiol. Int. 23 (6), 1139–1147.
- Forger, D.B., Jewett, M.E., Kronauer, R.E., 1999. A simpler model of the human circadian pacemaker. J. Biol. Rhythms 14, 532–537.
- Franken, Paul, Dudley, Carol A., Estill, Sandi Jo, Barakat, Monique, Thomason, Ryan, O'Hara, Bruce F., McKnight, Steven L., 2006. Npas2 as a transcriptional regulator of non-rapid eye movement sleep: genotype and sex interactions. Proc. Natl. Acad. Sci. USA, 103 (18), 7118–7123..
- Gleit, R.D., Diniz Behn, C., Booth, V., 2013. Modeling interindividual differences in spontaneous internal desynchrony patterns. J. Biol. Rhythms 28, 339–355.
- Gordon, Christopher J., Comas, Maria, Postnova, Svetlana, Miller, Christopher B., Roy, Dibyendu, Bartlett, Delwyn J., Grunstein, Ronald R., 2018. The effect of consecutive transmeridian flights on alertness, sleep-wake cycles and sleepiness: a case study. Chronobiol. Int. 35 (11), 1471–1480.
- Huang, Z.L., Urade, Y., Hayaishi, O., 2007. Prostaglandins and adenosine in the regulation of sleep and wakefulness. Curr. Opin. Pharmacol. 7, 33–38.
- Jaggard, James B., Stahl, Bethany A., Lloyd, Evan, Prober, David A., Duboue, Erik R., Keene, Alex C., 2018. Hypocretin underlies the evolution of sleep loss in the mexican cavefish. Elife 7, 02.

- Sat Bir, S., Khalsa, Deirdre A., Conroy, Jeanne F., Duffy, Charles, Czeisler, A., Dijk, Derk-Jan, 2002. Sleep- and circadian-dependent modulation of rem density. J. Sleep Res. 11 (1), 53–59.
- Knutson, Kristen L., Spiegel, Karine, Penev, Plamen, Van Cauter, Eve, 2007. The metabolic consequences of sleep deprivation. Sleep Med. Rev., 11(3), 163–178.
- Kronauer, R.E., Forger, D.B., Jewett, M.E., 1999. Quantifying human circadian pacemaker response to brief, extended, and repeated light stimuli over the photopic range. J. Biol. Rhythms 14, 501–515.
- Kumar, R., Bose, A., Mallick, B.N., 2012. A mathematical model towards understanding the mechanism of neuronal regulation of wake-NREMS-REMS states. PLoS One 7, e2059.
- Leung, Louis C., Mourrain, Philippe, 2018. Sleep: Short sleepers should keep count of their hypocretin neurons. Curr. Biol. 28 (9), R558–R560.
- Mallis, M.M., Mejdal, S., Nguyen, T.T., Dinges, D.F., 2004. Summary of the key features of seven biomathematical models of human fatigue and performance. Aviat. Space Environ. Med. 75 (3), A4–A14.
- Morairty, Stephen R., Dittrich, Lars, Pasumarthi, Ravi K., Valladao, Daniel, Heiss, Jaime E., Gerashchenko, Dmitry, Kilduff, Thomas S., 2013. A role for cortical nnos/nk1 neurons in coupling homeostatic sleep drive to eeg slow wave activity. Proc. Natl. Acad. Sci. 110 (50), 20272–20277.
- Mullington, Janet M., Haack, Monika, Toth, Maria, Serrador, Jorge M., Meier-Ewert, Hans K., 2009. Cardiovascular, inflammatory, and metabolic consequences of sleep deprivation. Prog. Cardiovasc. Dis. 51 (4), 294–302.
- Myers, C.R., Gutenkunst, R.N., Sethna, J.P., 2007. Python unleashed on systems biology. Comput. Sci. Eng. 9 (3).
- Phillips, A.J.K., Robinson, P.A., 2007. A quantitative model of sleep-wake dynamics based on the physiology of the brainstem ascending arousal system. J. Biol. Rhythms 22, 167–179.
- Phillips, A.J.K., Robinson, P.A., 2008. Sleep deprivation in a quantitative physiologically based model of the ascending arousal system. J. Theor. Biol. 255, 413–423.
- Postnova, Svetlana, Layden, Andrew, Robinson, Peter A., Phillips, Andrew J.K., Abeysuriya, Romesh G., 2012 Exploring sleepiness and entrainment on permanent shift schedules in a physiologically based model. J. Biol. Rhythms, 27(1), 91–102...
- Postnova, Svetlana, Lockley, Steven W., Robinson, Peter A., 2016. Sleep propensity under forced desynchrony in a model of arousal state dynamics. J. Biol. Rhythms, 31(5), 498–508...
- Postnova, Svetlana, Lockley, Steven W., Robinson, Peter A., 2018. Prediction of cognitive performance and subjective sleepiness using a model of arousal dynamics. J. Biol. Rhythms, 33(2), 203–218..
- Postnova, Svetlana, Postnov, Dmitry D., Seneviratne, Martin, Robinson, Peter A., 2014. Effects of rotation interval on sleepiness and circadian dynamics on forward rotating 3-shift systems. J. Biol. Rhythms, 29(1), 60–70.
- Rempe, M.J., Best, J., Terman, D., 2010. A mathematical model of the sleepwake cycle. J. Math. Biol. 60, 615–644.
- Rusterholz, T., Durr, R., Achermann, P., 2010. Inter-individual differences in the dynamics of sleep homeostasis. Sleep 33, 491–498.
- Sakurai, Takeshi, 2007. The neural circuit of orexin (hypocretin): maintaining sleep and wakefulness. Nat. Rev. Neurosci. 8 (3), 171–181.
- Saper, C.B., Chou, T.C., Scammell, T.E., 2001. The sleep switch: hypothalamic control of sleep and wakefulness. Trends Neurosci. 24, 726–731.
- Serkh, K., Forger, D.B., 2014. Optimal schedules of light exposure for rapidly correcting circadian misalignment. PLoS Comput. Biol. 10, e1003523.
- Tobaldini, Eleonora, Costantino, Giorgio, Solbiati, Monica, Cogliati, Chiara, Kara, Tomas, Nobili, Lino, Montano, Nicola, 2017. Sleep, sleep deprivation, autonomic nervous system and cardiovascular diseases. Neurosci. Biobehav. Rev. 74 (Pt B), 321–329.
- Van Dongen, H., Maislin, G., Mullington, J.M., Dinges, D.F., 2003. The cumulative cost of additional wakefulness: dose-response effects on neurobehavioral functions and sleep physiology from chronic sleep restriction and total sleep deprivation. Sleep 26 (2), 117–126.
- Van Dongen, H.P.A., Vitellaro, K.M., Dinges, D.F., 2005. Individual differences in adult human sleep and wakefulness: Leitmotif for a research agenda. Sleep 28 (4), 479–498.